MedChemComm

CONCISE ARTICLE

View Article Online
View Journal | View Issue

Published on 12 August 2014. Downloaded by Reprints Desk on 8/12/2024 6:47:55 PM.

Cite this: *Med. Chem. Commun.*, 2014, **5**, 1700

# Selective inhibitors of fibroblast activation protein (FAP) with a xanthine scaffold†

Koen Jansen,[a] Hans De Winter,[a] Leen Heirbaut,[a] Jonathan D. Cheng,[b] Jurgen Joossens,[a] Anne-Marie Lambeir,[c] Ingrid De Meester,[c] Koen Augustyns[a] and Pieter Van der Veken*[a]

Received 14th April 2014
Accepted 12th August 2014

DOI: 10.1039/c4md00167b

www.rsc.org/medchemcomm

Fibroblast activation protein (FAP) is a serine protease that is selectively expressed in many diseases involving activated stroma, including cancer, arthritis and hepatic and pulmonary fibrosis. FAP is closely related to dipeptidyl peptidase IV (DPPIV), of which many inhibitors are known and several are marketed as drugs. One of these is the xanthine derivative linagliptin. In a broad literature screen amongst reported DPPIV inhibitors, linagliptin was the only druglike compound identified that possessed significant FAP potency. Hence, this compound served as a starting point for a SAR study that aimed to identify structural determinants that selectively increase FAP-potency of linagliptin analogues. By investigating the influence of the substitution pattern on N1, N7 and C8 of the xanthine scaffold, we managed to decouple DPPIV and FAP potency and identified the first selective xanthine-based FAP inhibitors with low micromolar potency. Furthermore, these compounds are the only known FAP-inhibitors that do not rely on a warhead functionality to obtain potencies in this range.

## Introduction

Fibroblast activation protein (FAP, FAP-α, seprase) is a prolyl specific serine protease, closely related to the dipeptidyl peptidases (DPPs) DPPIV, DPP8/9 and DPP II. In addition, it is also phylogenetically linked to prolyl oligopeptidase (PREP). FAP has dual endopeptidase and dipeptidyl-peptidase activity.[1] It is expressed on activated stromal fibroblasts and pericytes of 90% of common human epithelial tumors examined.[2,3] Its function in tumors has been related to extracellular matrix degradation, tumor immune recognition and angiogenesis.[4] FAP is also expressed on activated fibroblasts in other tissues with extracellular matrix remodeling such as those present in cirrhosis, fibrotic diseases, rheumatoid arthritis, keloidosis and glioblastoma.[5–11] Interestingly, FAP is generally not expressed in normal, healthy adult tissues apart from granulation tissue during wound repair.[12]

Inhibition of FAP in mouse cancer models has been shown to attenuate tumor growth.[13,14] Furthermore, several studies are currently ongoing that investigate the effect of FAP-inhibition in other diseases characterised by FAP expression. Most of the previously reported FAP inhibitors have a dipeptide-derived architecture and bind covalently to the catalytic serine of the enzyme *via* an electrophilic warhead.[15–17] Relevant examples of such compounds include Val-*boro*Pro (**1**), a potent but non-selective inhibitor of the dipeptidyl peptidase family and UAMC-01110 (**2**), a low nanomolar, selective cyanopyrrolidine inhibitor of FAP that we reported recently[18,19] (Fig. 1, Table 1).

Other notable examples from recent literature include a structurally distinct series of 2-cyanopyrrolidines reported by Jiaang *et al.* and novel, optimized *boro*Pro inhibitors published by Poplawski *et al.*[20,21]

Within the dipeptidyl peptidase family, the clinically validated drug target DPPIV shows the highest resemblance to FAP. Both have highly comparable catalytic domain structures, characterized by 70% amino acid similarity. This feature is most

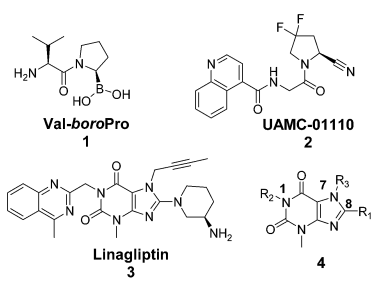


Fig. 1 Structure of reference inhibitors used (**1–3**) and the general structure of the target compounds in this study (**4**).

[a]*Medicinal Chemistry (UAMC), Department of Pharmaceutical Sciences, University of Antwerp (UA), Universiteitsplein 1, B-2610 Antwerp, Belgium. E-mail: pieter.vanderveken@uantwerpen.be*

[b]*Fox Chase Cancer Center, 333 Cottman Avenue, Philadelphia PA-19111-2497, USA*

[c]*Medical Biochemistry, Department of Pharmaceutical Sciences, University of Antwerp (UA), Universiteitsplein 1, B-2610 Antwerp, Belgium*

† Electronic supplementary information (ESI) available: Detailed synthesis protocols and analytical data for the compounds. See DOI: 10.1039/c4md00167b



This journal is © The Royal Society of Chemistry 2014

Johns Hopkins University EX2003
GE Healthcare v. Johns Hopkins
PGR2025-00059

Published on 12 August 2014. Downloaded by Reprints Desk on 8/12/2024 6:47:55 PM.

Table 1 $IC_{50}$-values for reference compounds **1–3**

| Nr | FAP | $IC_{50}$ (μM) DPP IV | PREP | DPP9 | DPP II |
|---|---|---|---|---|---|
| **1** | 0.07 ± 0.01 | 0.022 ± 0.001 | 0.98 ± 0.06 | N.D.[a] | 0.086 ± 0.007 |
| **2** | 0.0033 ± 0.0004 | >100 | 1.8 ± 0.2 | >12.5 | >100 |
| **3** | 0.37 ± 0.002 | 0.0020 ± 0.0002 | >100 | >100 | >100 |

[a] N.D. = not determined.

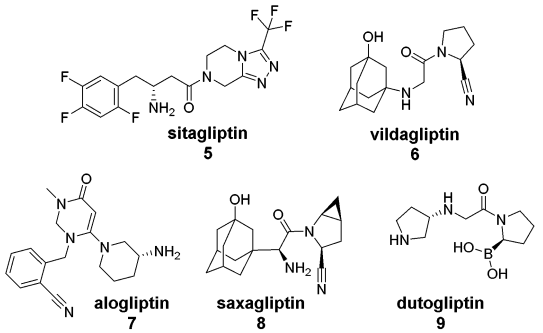


Fig. 2 Structures of clinically relevant DPP IV inhibitors with reported FAP-affinities.

pronounced in their active sites, where the only significant difference between both is the presence of Ala657 in FAP, instead of DPPIV's Asp663 (Fig. 3, entry (a)).[17] Therefore, we reasoned that known DPPIV inhibitors could form valid starting points for discovery of, or for reverse engineering into FAP inhibitors. Upon review of the literature, we found that the FAP potency of a significant fraction of all reported DPPIV inhibitors has not been investigated or disclosed. Nonetheless, owing to the fact that very large numbers of DPPIV inhibitors have been published to date, we were still able to find a substantial number of compounds with reported FAP affinities. Examples of these that were investigated clinically and represent most of the important DPP IV inhibitor chemotypes are shown in Fig. 2. Of the approved DPPIV inhibitors, linagliptin and saxagliptin were the only examples with notable, reported FAP-potency (Table 2). The dipeptide derived saxagliptin (**8**) has been described to possess micromolar FAP-affinity. Linagliptin (**3**) however, has approximately tenfold higher, submicromolar FAP potency. In addition, linagliptin possesses excellent selectivity towards the related peptidases DPP8/9 and PREP. In earlier reports, we and others have stressed the importance of finding selective FAP inhibitors, most specifically with respect to the endopeptidase PREP.[16,17,19]

Its selectivity profile, together with its straightforward synthesis and proven druglike properties, in our opinion clearly justified the selection of linagliptin as a starting point for discovery of FAP inhibitors. We also identified a patent application by researchers from Boehringer Ingelheim, claiming the application in FAP-related diseases of compounds that are structurally very close to linagliptin.[26] This document however did not include FAP-affinities for the molecules proposed, nor

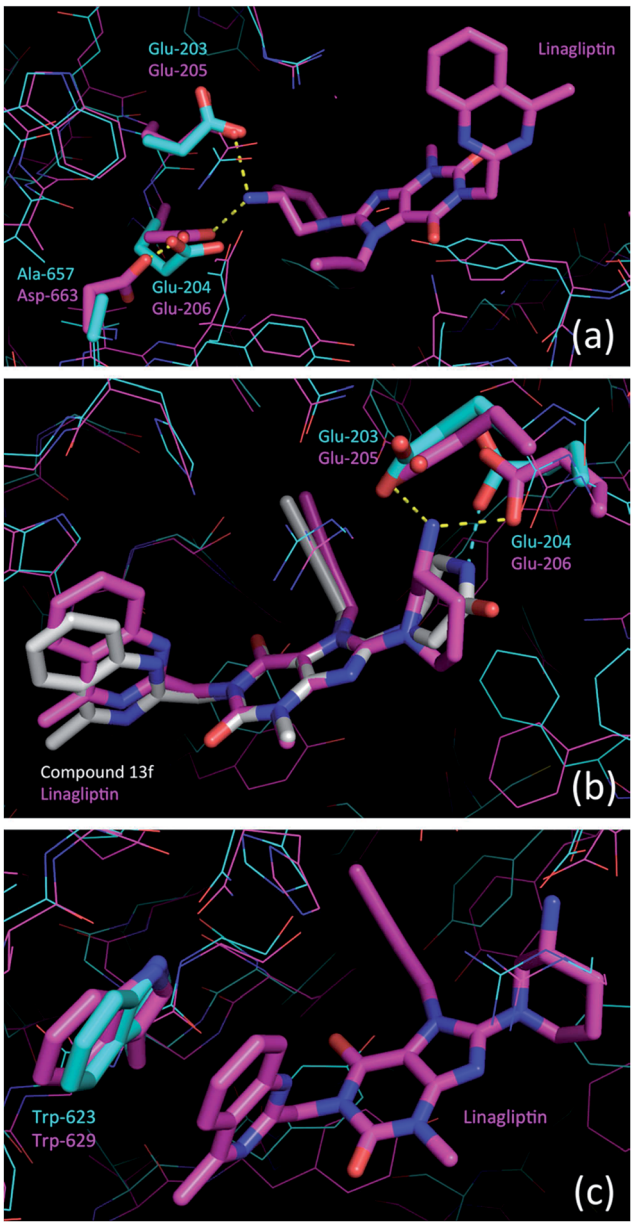


Fig. 3 Overview of key modeling results, obtained using the co-crystal structure of DPP IV and linagliptin (pdb-entry: 2RGU, purple-colored atoms) and the crystal structure of FAP (pdb-entry: 1Z68, cyan-colored atoms).[1,28] Potential hydrogen bonds are represented using dotted lines. All data were obtained using MOE, version 2013.08 and PyMOL.[31,32] Entry (a) linagliptin in DPP IV's active center overlaid with the corresponding part of FAP. Residues assumed to be responsible for the different ligand selectivities of both enzymes are highlighted. Entry (b) superposition of linagliptin in DPP IV's active center and compound 13f (grey atoms), docked in FAP's active center. This image illustrates the possibility of a stabilizing interaction between 13f's piperazinone-NH and FAP's Glu204. Entry (c): linagliptin in DPP IV's active center overlaid with the corresponding part of FAP. The homologous Trp-residues of DPP IV and FAP, assumed to be engaged in stacking interactions with linagliptin's methylquinazoline ring are highlighted.

selectivity data with respect to DPP IV. Our study therefore represents the first reported systematic investigation of the substituents decorating the 1-,7- and 8-positions of the xanthine

Published on 12 August 2014. Downloaded by Reprints Desk on 8/12/2024 6:47:55 PM.

Table 2 Literature potency and selectivity data of DPP IV inhibitors that have been investigated clinically

| | $IC_{50}$ (μM) | | | | | | |
|---|---|---|---|---|---|---|---|
| Nr | FAP | DPPIV | PREP | DPP8 | DPP9 | DPPII | Ref. |
| **3** (Linagliptin)[a] | 0.089 | 0.001 | >100 | >40 | >100 | >100 | 22 |
| **5** (Sitagliptin) | >100 | 0.012 | >100 | 19 | 62 | >100 | 23 |
| **6** (Vildagliptin) | 73 | 0.023 | >50 | 1.4 | 0.08 | >100 | 23 |
| **7** (Alogliptin) | >100 | 0.0069 | >100 | >100 | >100 | >100 | 23 |
| **8** (Saxagliptin) | 2.6 | 0.001 | >100 | 0.197 | 0.054 | N.R.[b] | 24 |
| **9** (Dutogliptin) | 7.52 | 0.023 | N.R. | 8.427 | 0.663 | >0.4 | 25 |

[a] Data reported in ref. 21; $IC_{50}$-values for linagliptin determined in this work are shown in Table 1. [b] N.R. = not reported.

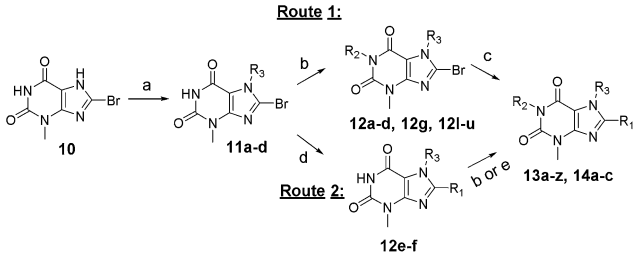


Scheme 1 Synthesis of target compounds **13a–z** and **14a–c**. Reagents and conditions: (a) $R_3$-Br, DIPEA, DMF, 80 °C; (b) $R_2$-X, $K_2CO_3$, DMF, 65 °C; (c) $R_1H$, $K_2CO_3$, DMF, 50 °C; (d) $Et_3N$, piperazin-2-one, *N*,*N*-dimethylacetamide, 75 °C, 6 h; (e) $R_2$-X, LiH, DMF, rt.

scaffold of linagliptin with the aim of finding structural features determining FAP or DPPIV affinity. Around thirty novel compounds were designed and synthesized aiming to extract a maximal amount of SAR information. The general structure of these compounds is represented by compound **4** (Fig. 1).

For the design of these molecules, we first turned our attention to the C8-position, which bears a protonatable amine group in linagliptin. The latter mimicks the free amino-terminus of DPPIV's peptide substrates and is known to be an essential part of the typical dipeptidyl-peptidase pharmacophore. Based on FAP's endopeptidase capability, we hypothesized the basic amine not to be necessary for potency on this enzyme.[15] Therefore, we included in our series of linagliptin analogues a significant number of molecules bearing non-basic residues at this position ($R_1$ in structure **4**, Fig. 1). In this series of molecules, the 4-methylquinazoline-($R_2$) and 2-butyn-1-yl-($R_3$) groups present in linagliptin were conserved, to allow efficient comparison of the novel molecules with the parent reference structure. It deserves mentioning also that the 4-methylquinazoline N1 substituent has been indicated as contributing to the FAP-affinity of both linagliptin and a 7-cyanodeazapurine analogue, another argument justifying its selection for this initial compound series.[27]

In a second series of molecules, the 4-methylquinazoline substituent ($R_2$) of the xanthine scaffold was varied. Several analogues and other mono- and bicyclic (hetero-)aromatic systems were selected for introduction. These were supplemented with the butynyl residue ($R_3$) of linagliptin and one of the optimal $R_1$-residues was identified in the first series of compounds, likewise to allow efficient comparison between modified and parent structures.

Our SAR study was concluded with the investigation of a number of lipophilic N7-substituents ($R_3$) which were expected to bind in the S1 pocket of FAP, similar to linagliptin's butynyl-residue. These $R_3$-substituents were again combined with optimal $R_1$ and $R_2$ substituents discovered in the foregoing steps.

## Synthesis

The synthesis of all reported compounds was performed starting from 8-bromo-3-methylxanthine **10**, using the methodology described earlier for the parent compound linagliptin[28] (Scheme 1). Using this strategy, substituents on N7 ($R_2$) and N1 ($R_3$) of the xanthine scaffold can be introduced in a regioselective manner by exploiting intrinsic differences in alkylation reactivity between both positions. The C8-substituent ($R_1$) is introduced *via* $S_NAr$ on the brominated C8 position of the xanthine scaffold.

Practically, the N7 position of starting material **10** was alkylated first with a series of alkyl halides in the presence of $K_2CO_3$ to yield intermediates **11a–d**. These were then further derivatized at the N1 position with a different series of alkyl halides and $K_2CO_3$ in DMF to give the N1/N7 doubly derivatized analogs **12a–d**, **12g** and **12l–u** (Scheme 1, Route 1). The final compounds were therefore obtained by nucleophilic displacement of the C8 bromine group with a series of amines. Alternatively, for several final compounds with a 1-(piperazin-3-onyl-) substituent at C8 (*vide infra*), nucleophilic aromatic substitution was performed first to obtain **12e** and **12f** (Scheme 1, Route 2). Alkylation of N1 using the corresponding alkyl halides was carried out as the last step. This strategy was found to be largely equivalent to the one described under "Route 1".

### Biochemical evaluation

For all inhibitors produced, the affinities toward FAP, DPPIV, DPP9, DPP II and PREP were evaluated. Affinities toward DPP8 were not determined for individual compounds: due to the high degree of homology between DPP8 and DPP9 (overall sequence identity: 57%; active site sequence identity: 90%) and based on findings we reported earlier, affinities for both enzymes can be expected to be generally comparable.[29] Overall, compounds synthesized were found to be devoid of significant affinity ($IC_{50}$ > 100) with respect to DPP9, DPP2 and PREP with the notable exception of compound **13s**, which was found to have low micromolar DPP9 potency.

## Results and discussion

Table 3 summarizes the results obtained for the first series of molecules, in which the C8-substituent ($R_1$) was varied. For the reasons explained earlier, emphasis was put on the introduction of non-basic $R_1$ residues at this position. Only piperazine derivatives **13a** and **13b** do not belong to this group. The

 This journal is © The Royal Society of Chemistry 2014

Published on 12 August 2014. Downloaded by Reprints Desk on 8/12/2024 6:47:55 PM.

Table 3 C8-substituted xanthines

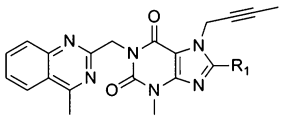

| | | $IC_{50}$ (μM) | | | | |
|---|---|---|---|---|---|---|
| Nr | $R_1$ | FAP | DPP IV | PREP | DPP9 | DPPII |
| **3** | 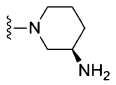 (Linagliptin) | 0.37 ± 0.02[a] | 0.0020 ± 0.0002 | >100 | >100 | >100 |
| **13a** | 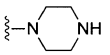 | 0.74 ± 0.04[a] | 0.0194 ± 0.0021 | >100 | >100 | >100 |
| **13b** | 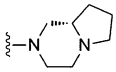 | 11 ± 1 | 13.9 ± 0.8 | >100 | >100 | >100 |
| **13c** | | >10 | >100 | >100 | >100 | >100 |
| **13d** | | >100 | >100 | >100 | >100 | >100 |
| **13e** | 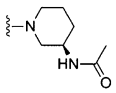 | >10 | 12.2 ± 0.7 | >100 | >100 | >100 |
| **13f** | 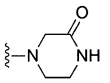 | 1.9 ± 0.1 | >50 | >100 | >100 | >100 |
| **13g** | 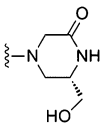 | 3.3 ± 0.5 | 18.1 ± 0.9 | >100 | >100 | >100 |
| **13h** | 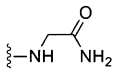 | >100 | >100 | >100 | >100 | >100 |
| **13i** | 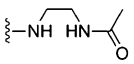 | >10 | >100 | >100 | >100 | >100 |
| **13j** | 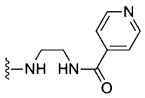 | >10 | >50 | >100 | >100 | >100 |

[a] Average of two independent measurements.

piperazine ring in **13a** was selected based on early work toward the discovery of linagliptin. There, a C8-piperazine ring was found to be significantly less desirable for DPP IV potency than linagliptin's aminopiperidine system. In a crystallographic study of a related xanthine by Engel *et al.*, the energetically unfavourable twist conformation the piperazine ring adopts in such a way to allow interaction with DPPIV's Glu205-Glu206 motif, was proposed as a possible rationale for this observation.[30] The roughly tenfold drop in DPP IV affinity that we indeed observed, was however also found to be accompanied by a drop in FAP affinity, though the latter in a more modest fashion. Nonetheless, although slightly less selective, **13a** is still mainly a DPP IV inhibitor. Introduction of the more sterically demanding tertiary piperazine derivative in **13b** nivellates FAP and DPP IV potencies, but also further reduces affinity for both targets. In the non-basic C8 substituent series, a drastic, near-complete loss of affinity for both target enzymes was observed upon removal of the amine function, as in piperidine **13c**. These data indicate that the amine functions of linagliptin or **13a** are also involved in binding to FAP's active center, most likely by interacting with FAP's Glu203–Glu204 motif, which is homologous to the Glu205–Glu206 motif in DPP IV. We therefore turned to substituent types that contain amide groups in the same position, hypothesizing that such motifs would mimick

Published on 12 August 2014. Downloaded by Reprints Desk on 8/12/2024 6:47:55 PM.

the P2–P3 peptide bond recognized by FAP in its endopeptidase substrates. Although not capable of ionic interactions, amides can still be involved in, *e.g.*, dipole-dipole interactions or hydrogen bonding with Glu203–Glu204. We confirmed this possibility *via* molecular docking (*vide supra*), although it should be mentioned that the exact nature of the interaction (presumed important for recognition of FAP's endopeptidase substrates) has not been characterised experimentally. Structural studies nonetheless have explained the differences in substrate recognition patterns between FAP and DPP IV by emphasizing the slightly different orientations of the Glu–Glu motifs in both enzymes, and have pointed at the presence of Ala657 in FAP *versus* Asp663 in DPP IV as the direct cause of these differences.

The *N*-acetylated derivative of linagliptin **13e** was prepared to serve as a straightforward proof-of-concept inhibitor for this hypothesis. It was found not to possess FAP potency but compared to the parent compound, its DPPIV potency had also been reduced over thousand-fold. Introduction of the amide's oxo function on a piperazine ring (as in piperazinones **13f** and **13g**) yielded better results, with unsubstituted piperazinone **13f** combining optimal FAP-potency and selectivity with respect to DPP IV. Although there seems to be room for further optimization of its potency, this molecule is the first selective FAP inhibitor that does not rely on an electrophilic warhead to reach low micromolar potency and, in addition, does not have a peptide-derived overall architecture. Subsequently several more flexible amide analogues than piperazinone were introduced at C8 (compounds **13h** and **13i**). The main rationale for this was our supposition that the conformationally constrained piperazinone ring could have a subdued interaction with the enzyme's Glu–Glu motif. To shed additional light on this issue, a docking study for compound **13f** was carried out This study nonetheless indicated that hydrogen bonding between **13f's** piperazinone-NH and FAP's Glu204, but not FAP's Glu203 residue, could theoretically be present with a near strainless conformation of the piperazinone ring (Fig. 3, entry (b)). Furthermore, to investigate whether further optimisation on the presumed P3-mimicking side of the inhibitor would be possible, we introduced a 4-pyridinoyl substituent in **13j**. The latter is a determining part of an S3-binding pharmacophore for FAP that we described earlier.[18] None of the modifications present in **13h–13j**, led to further optimised FAP inhibitors. In the absence of direct structural clues for further optimization of the $R_1$ group, further expansion of this series was not planned at this point. We decided to select the piperazinone, piperazine and the (*R*)-aminopiperazine moieties and to conserve them in compounds designed to extract FAP-SAR information on the N1-substituent of the xanthine scaffold.

In the N1-varied series, compounds **13k–13n** contain bicyclic replacements for linagliptin's 4-methylquinazoline fragment (Table 4). Removal of the methyl group as in the quinazoline derivative **13k**, yields a compound that despite its piperazine C8-substituent, is a strong DPPIV inhibitor. Its potency for FAP however, decreases compared to both linagliptin and to the most closely related reference **13a**. 4-Methoxyquinazoline **13l** has similar FAP potency but, although 5-fold less, also still considerable DPPIV potency. Introduction of a mono-azaheteroaromatic quinoline ring in **13m** was found to reduce both FAP and DPPIV potency tenfold compared to the quinazoline-based **13k**, and thus neither improves affinity nor selectivity in FAP's advantage. Additional removal of the remaining $R_2$ heteroaromatic nitrogen atoms in the naphthyl derived **13n** proved even more deleterious both to FAP and DPPIV potency.

These results seem to indicate that in the bicyclic $R_2$-series, FAP and DPP IV potencies move along similar SAR trajectories. In the crystal structure of linagliptin in complex with DPPIV (PDB entry 2RGU), the two nitrogen heteroatoms of methylquinazoline form hydrogen bonds with co-crystallized water molecules but are not engaged in typical, strong affinity conferring interactions with the enzyme.[28] The phenyl part of the methylquinazoline on the other hand, is involved in a π–π interaction with DPPIV's Trp629. This interaction can be expected to be sensitive to changes in the overall electron density distribution of the aromatic system, and the latter might offer a rationale for the effects observed upon removal of ring nitrogens from the quinazoline system. Taking into account that in FAP's crystal structure, the homologous Trp623 residue occupies comparable parts of space as Trp629 in DPPIV, one might therefore conclude that selecting N1-substituents related to quinazoline does not offer a straightforward strategy to discriminate between FAP and DPPIV.[1] This hypothesis is illustrated in Fig. 3, entry (c). Therefore, we selected a number of aromatic and azaheteroaromatic $R_2$-substituents that are structurally and electronically more distant from the initial 4-methylquinazoline system of linagliptin (**13o–y**). The choice for these residues was driven partially by the desire to introduce more structural variation at N7 of the xanthine scaffold (compounds **13o–u** and **13y**). In addition, the pyridine containing series **13v–x**, was designed to further investigate the possibility of specific interactions of FAP with ring nitrogen heteroatoms, regardless of earlier hypotheses based on FAP/DPPIV homology. With this respect, the DPPIV-affinity excluding piperazinone moiety was immediately selected as the $R_1$ group in these inhibitors. None of the prepared compounds however, demonstrated notable affinity toward FAP. Therefore, no other analogues were planned in this series and we moved our focus to the potential of the $R_3$ substituent to improve FAP potency and selectivity.

To allow efficient comparison during the optimization of the $R_3$ substituent, the piperazinone and 4-methoxyquinazoline residues (present in **13l**) were selected as $R_1$ and $R_2$ groups in all compounds produced. Prior to this effort however, several "stripped" analogues were prepared to quantify the relative contributions of $R_2$ and $R_3$ to FAP potency (Table 5). Bearing in mind that a piperazinone $R_1$ group at this point was our only warrant for FAP selectivity, this substituent was considered a fixed element of all future analogues prepared. Therefore, careful weighing of the relative importance of $R_2$ and $R_3$ was considered mandatory to guide any extended optimization effort. From the data obtained with compounds **12e** and **f**, **13z** and **14a**, it is clear that both suitable $R_2$ and $R_3$ groups are required for FAP-potency within this series. In addition, these results indicate that the piperazinone moiety itself does not

 This journal is © The Royal Society of Chemistry 2014

Published on 12 August 2014. Downloaded by Reprints Desk on 8/12/2024 6:47:55 PM.

Table 4 N1-substituted xanthines

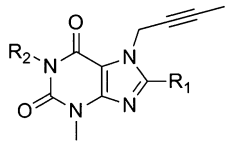

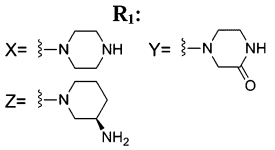


| | | | $IC_{50}$ (μM) | | | | |
|---|---|---|---|---|---|---|---|
| Nr | $R_2$ | $R_1$ | FAP | DPP IV | PREP | DPP9 | DPPII |
| **13k** | 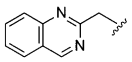 | X | 1.8 ± 0.1 | 0.0058 ± 0.0005 | >100 | >100 | >100 |
| **13l** | 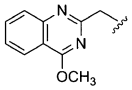 | X | 1.2 ± 0.1 | 0.025 ± 0.002 | >100 | >100 | >100 |
| **13m** | 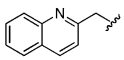 | X | 10.3 ± 0.4 | 0.029 ± 0.002 | >100 | >100 | >100 |
| **13n** | 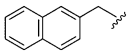 | X | 41 ± 2.2 | 0.18 ± 0.01 | >100 | >100 | >100 |
| **13o** | 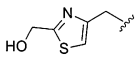 | X | >100 | 0.65 ± 0.03 | >100 | >100 | >100 |
| **13p** | | X | >100 | 1.23 ± 0.05 | >100 | >100 | >100 |
| **13q** | 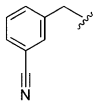 | X | >100 | 0.34 ± 0.01 | >100 | >100 | >100 |
| **13r** | 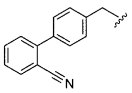 | X | >100 | 1.8 ± 0.1 | >100 | >100 | >100 |
| **13s** | 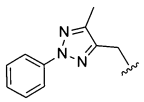 | X | >100 | 0.18 ± 0.01 | >100 | 6.3 ± 0.5 | >100 |
| **13t** | 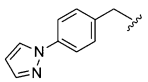 | X | >50 | 1.44 ± 0.04 | >100 | >100 | >100 |
| **13u** | 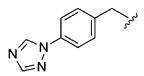 | X | >100 | 0.22 ± 0.01 | >100 | >100 | >100 |
| **13v** | | Y | >12.5 | >100 | >100 | >100 | >100 |
| **13w** | | Y | >100 | >100 | >100 | >100 | >100 |
| **13x** | | Y | >100 | >100 | >100 | >100 | >100 |
| **13y** | | Z | >100 | 0.98 ± 0.06 | >100 | >100 | >100 |

produce net added value in its interaction with the FAP's active center, and hence mainly serves as a selectivity enhancing moiety.

Subsequently, inhibitors containing an isopent-2-enyl, an isohex-2-enyl or a benzyl type $R_3$ group were prepared (Table 6). The choice for these fragments was also based on early work leading to linagliptin's discovery, where they were identified as suboptimal for rendering high DPPIV potency.[28] We found the corresponding compounds however to possess limited solubility, even in pure DMSO. Therefore $IC_{50}$ measurements of **14b**

Published on 12 August 2014. Downloaded by Reprints Desk on 8/12/2024 6:47:55 PM.

Table 5 Analogues devoid of $R_2$ and/or $R_3$ groups

| | | $IC_{50}$ (μM) | | | | |
|---|---|---|---|---|---|---|
| Nr | Structure | FAP | DPP IV | PREP | DPP9 | DPP II |
| **12f** | 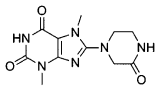 | >100 | >100 | >100 | >100 | >100 |
| **12e** | 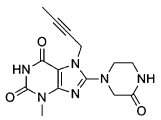 | >100 | >100 | >100 | >100 | >100 |
| **13z** | 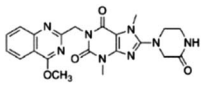 | >100 | >100 | >100 | >100 | >100 |
| **14a** | 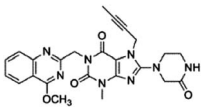 | 5.8 ± 0.5 | >100 | >100 | >100 | >100 |

Table 6 N7-diversified analogues

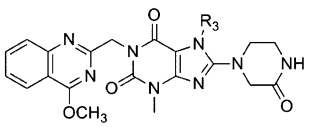

| | | $IC_{50}$ (μM) | | | | |
|---|---|---|---|---|---|---|
| Nr | $R_3$ | FAP | DPP IV | PREP | DPP9 | DPPII |
| **14b** | | N.D.[a] | N.D. | >100 | >100 | >100 |
| **14c** | | >50 | >100 | >100 | >100 | >100 |
| **14d** | | N.D. | N.D. | >100 | >100 | >100 |

[a] N.D. = Not determined; the $IC_{50}$-values of these compounds could not be determined due to solubility problems at concentrations > 1 μM.

and **14d** were not possible. Overall the butynyl was the best N-7-substituent assayed, suggesting that finding $R_3$-moieties with divergent FAP and DPP IV binding properties is far from evident.

## Conclusions

These data indicate that the SAR of xanthine inhibitors related to linagliptin is largely analogous for FAP and DPPIV, a finding that reflects the close phylogenetic relationship of both proteases. During our investigations, we nonetheless managed to decouple DPPIV and FAP potencies by replacing linagliptin's C8-aminopiperidine substituent by a piperazinone ring. This led to the first selective FAP-inhibitors with a non-peptide derived overall architecture. Our best compounds (**13f** and **g**, **14a**) displayed affinities in the low micromolar range and are the first FAP-inhibitors that attain this potency range without relying on an electrophilic warhead function. Since the piperazinone ring itself does not seem to contribute significantly to the observed potency, further optimization of these molecules is expected to comprise extended exploration of the chemical space around the N1 and N7 substituents. Furthermore, scaffold modification or substitution of the piperazinone system could be investigated to probe for additional interactions with FAP.

## Acknowledgements

We thank Nicole Lamoen and Sophie Lyssens for excellent technical assistance.

## Notes and references

1 K. Aertgeerts, I. Levin, L. Shi, G. P. Snell, A. Jennings, G. S. Prasad, Y. Zhang, M. L. Kraus, S. Salakian, V. Sridhar, R. Wijnands and M. G. Tennant, *J. Biol. Chem.*, 2005, **280**, 19441–19444.
2 P. Garin-Chesa, L. J. Old and W. J. Rettig, *Proc. Natl. Acad. Sci. U. S. A.*, 1990, **87**, 7235–7239.
3 M. J. Scanlan, B. K. Raj, B. Calvo, P. Garin-Chesa, M. P. Sanz-Moncasi, J. H. Healey, L. J. Old and W. J. Rettig, *Proc. Natl. Acad. Sci. U. S. A.*, 1994, **91**, 5657–5661.
4 W. N. Brennen, J. T. Isaacs and S. R. Denmeade, *Mol. Cancer Ther.*, 2012, **11**, 257–266.
5 X. M. Wang, T.-W. Yao, N. A. Nadvi, B. Osborne, G. W. McCaughan and M. D. Gorrell, *Front. Biosci.*, 2008, **13**, 3168–3180.
6 P. S. Acharya, A. Zukas, V. Chandan, A. L. Katzenstein and E. Pure, *Hum. Pathol.*, 2006, **37**, 352–360.
7 J. M. Milner, L. Kevorkian, D. A. Young, D. Jones, R. Wait, S. T. Donell, E. Barksby, A. M. Patterson, J. Middleton, B. F. Cravatt, I. M. Clark, A. D. Rowan and T. E. Cawston, *Arthritis Res. Ther.*, 2006, **8**, R23.
8 K. Dienus, A. Bayat, B. F. Gilmore and O. Seifert, *Arch. Dermatol. Res.*, 2010, **302**, 725–731.
9 S. Bauer, C. Ospelt and C. Renner, *Arthritis Rheum.*, 2010, **62**, 3514–3515.
10 S. Bauer, M. C. Jendro, A. Wadle, S. Kleber, F. Stenner, R. Dinser, A. Reich, E. Faccin, S. Gödde, H. Dinges, U. Müller-Ladner and C. Renner, *Arthritis Res. Ther.*, 2006, **8**, R171.
11 R. Mentlein, K. Hattermann, C. Hemion, A. a. Jungbluth and J. Held-Feindt, *Biol. Chem.*, 2011, **392**, 199–207.
12 M. T. Levy, G. W. McCaughan, C. A. Abbott, J. E. Park, A. M. Cunningham, E. Müller, W. J. Rettig and M. D. Gorrell, *Hepatology*, 1999, **29**, 1768–1778.
13 A. M. Santos, J. Jung, N. Aziz, J. L. Kissil and E. Puré, *J. Clin. Invest.*, 2009, **119**, 3613–3625.

 This journal is © The Royal Society of Chemistry 2014

Published on 12 August 2014. Downloaded by Reprints Desk on 8/12/2024 6:47:55 PM.

14 J. D. Cheng, M. Valianou, A. A. Canutescu, E. K. Jaffe, H.-O. Lee, H. Wang, J. H. Lai, W. W. Bachovchin and L. M. Weiner, *Mol. Cancer Ther.*, 2005, **4**, 351–360.
15 O. Ryabtsova, K. Jansen, S. Van Goethem, J. Joossens, J. D. Cheng, A.-M. Lambeir, I. De Meester, K. Augustyns and P. Van der Veken, *Bioorg. Med. Chem. Lett.*, 2012, **22**, 3412–3417.
16 B. B. Wolf, C. Quan, T. Tran, C. Wiesmann and D. Sutherlin, *Mini–Rev. Med. Chem.*, 2008, **8**, 719–727.
17 T. Tran, C. Quan, C. Y. Edosada, M. Mayeda, C. Wiesmann, D. Sutherlin and B. B. Wolf, *Bioorg. Med. Chem. Lett.*, 2007, **17**, 1438–1442.
18 K. Jansen, L. Heirbaut, J. D. Cheng, J. Joossens, O. Ryabtsova, P. Cos, L. Maes, A.-M. Lambeir, I. De Meester, K. Augustyns and P. Van der Veken, *ACS Med. Chem. Lett.*, 2013, **4**, 491–496.
19 K. Jansen, L. Heirbaut, R. Verkerk, J. D. Cheng, J. Joossens, P. Cos, L. Maes, A.-M. Lambeir, I. De Meester, K. Augustyns and P. Van der Veken, *J. Med. Chem.*, 2014, **57**, 3053–3074.
20 T.-Y. Tsai, T.-K. Yeh, X. Chen, T. Hsu, Y.-C. Jao, C.-H. Huang, J.-S. Song, Y.-C. Huang, C.-H. Chien, J.-H. Chiu, S.-C. Yen, H.-K. Tang, Y.-S. Chao and W.-T. Jiaang, *J. Med. Chem.*, 2010, **53**, 6572–6583.
21 (*a*) S. E. Poplawski, J. H. Lai, Y. Li, Z. Jin, Y. Liu, W. Wu, Y. Wu, Y. Zhou, J. L. Sudmeyer, D. G. Sandford and W. W. Bachovchin, *J. Med. Chem.*, 2013, **56**, 3467–3477; (*b*) W. W. Bachovchin, H.-S. Lai and W. Wu, WO2010099537, 2010.
22 (*a*) L. Thomas, M. E. Eckhardt, M. Langkopf, F. Tadayyon, F. Himmelsbach and M. Mark, *J. Pharmacol. Exp. Ther.*, 2008, **325**, 175–182; (*b*) L. Thomas, M. Eckhardt, E. Langkopf, M. Tadayyon and F. Himmelsbach, *Pharmacology*, 2008, **325**, 175–182.
23 B. Lee, L. Shi, D. B. Kassel, T. Asakawa, K. Takeuchi and R. J. Christopher, *Eur. J. Pharmacol.*, 2008, **589**, 306–314.
24 T.-K. Yeh, T.-Y. Tsai, T. Hsu, J.-H. Cheng, X. Chen, J.-S. Song, H.-S. Shy, M.-C. Chiou, C.-H. Chien, Y.-J. Tseng, C.-Y. Huang, K.-C. Yeh, Y.-L. Huang, C.-H. Huang, Y.-W. Huang, M.-H. Wang, H.-K. Tang, Y.-S. Chao, C.-T. Chen and W.-T. Jiaang, *Bioorg. Med. Chem. Lett.*, 2010, **20**, 3596–3600.
25 (*a*) C.-S. Lee, H. J. Yim, K.-H. Kim, J. Lee, S.-H. Lee, K. W. Lee, W. S. Park and C. Min, WO2009082134, 2009; (*b*) A. Marie, D. A. Campbell, D. T. Winn, D. Hanway, J. M. Cherrington, M. Mcneil, P. McNamara and X. Li, *Diabetes*, 2006, **55**(6 suppl 1), 538.
26 F. Himmelsbach, M. Mark, M. Tadayyon and L. Thomas, WO2009024542, 2009.
27 J. M. Sutton, D. E. Clark, S. J. Dunsdon, G. Fenton, A. Fillmore, N. V. Harris, C. Higgs, C. a. Hurley, S. L. Krintel, R. E. MacKenzie, A. Duttaroy, E. Gangl, W. Maniara, R. Sedrani, K. Namoto, N. Ostermann, B. Gerhartz, F. Sirockin, J. Trappe, U. Hassiepen and D. K. Baeschlin, *Bioorg. Med. Chem. Lett.*, 2012, **22**, 1464–1468.
28 M. Eckhardt, E. Langkopf, M. Mark, M. Tadayyon, L. Thomas, H. Nar, W. Pfrengle, B. Guth, R. Lotz, P. Sieger, H. Fuchs and F. Himmelsbach, *J. Med. Chem.*, 2007, **50**, 6450–6453.
29 S. Van Goethem, V. Mateeussen, J. Joossens, A. M. Lambeir, X. Chen, I. De Meester, A. Haemers, K. Augustyns and P. Van der Veken, *J. Med. Chem.*, 2011, **54**, 5737–5746.
30 M. Engel, T. Hoffmann, S. Manhart, U. Heiser, S. Chambre, R. Huber, H.-U. Demuth and W. Bode, *J. Mol. Biol.*, 2006, **355**, 768–783.
31 Molecular Operating Environment (MOE), version 2013.08; Chemical Computing Group Inc., 1010 Sherbooke St. West, Suite #910, Montreal, QC, Canada, H3A 2R7, 2013. Protein residues were kept fixed during all modeling experiments and were not changed compared to the parent crystal structures used.
32 'The PyMOL Molecular Graphics System', Version 1.5.0.4, Schrödinger, LLC; https://www.pymol.org.